Psychiatry Research: Neuroimaging 202 (2012) 118–125

Contents lists available at SciVerse ScienceDirect

Psychiatry Research: Neuroimaging

journal homepage: www.elsevier.com/locate/psychresns

Altered topological patterns of brain networks in mild cognitive impairment and Alzheimer's disease: A resting-state fMRI study

Zhenyu Liu [a,1], Yumei Zhang [b,1], Hao Yan [d,e], Lijun Bai [a], Ruwei Dai [a], Wenjuan Wei [a], Chongguang Zhong [a], Ting Xue [c], Hu Wang [a], Yuanyuan Feng [a], Youbo You [a], Xinghu Zhang [b], Jie Tian [a,c,*]

[a] Intelligent Medical Research Center, Institute of Automation, Chinese Academy of Sciences, Beijing, 100190, China
[b] Neurology department Beijing Tiantan Hospital, affiliated with Capital Medical University, 100050, China
[c] Life Science Research Center, School of Electronic Engineering, Xidian University, Xi'an, Shaanxi, 710071, China
[d] School of Psychology, Shaanxi Normal University, Xi'an 710062, China
[e] Department of Linguistics, Xidian University, Xi'an 710071, China

ARTICLE INFO

Article history:
Received 30 June 2011
Received in revised form 22 November 2011
Accepted 9 March 2012

Keywords:
Alzheimer's disease
Mild cognitive impairment
Functional MRI
Small-world network
Nodal centrality

ABSTRACT

Recent studies have shown that cognitive and memory decline in patients with Alzheimer's disease (AD) is coupled with losses of small-world attributes. However, few studies have investigated the characteristics of the whole brain networks in individuals with mild cognitive impairment (MCI). In this functional magnetic resonance imaging (fMRI) study, we investigated the topological properties of the whole brain networks in 18 AD patients, 16 MCI patients, and 18 age-matched healthy subjects. Among the three groups, AD patients showed the longest characteristic path lengths and the largest clustering coefficients, while the small-world measures of MCI networks exhibited intermediate values. The finding was not surprising, given that MCI is considered to be the prodromal stage of AD. Compared with normal controls, MCI patients showed decreased nodal centrality mainly in the medial temporal lobe as well as increased nodal centrality in the occipital regions. In addition, we detected increased nodal centrality in the medial temporal lobe and frontal gyrus, and decreased nodal centrality mainly in the amygdala in MCI patients compared with AD patients. The results suggested a widespread rewiring in AD and MCI patients. These findings concerning AD and MCI may be an integrated reflection of reorganization of the brain networks accompanied with the cognitive decline that may lead to AD.

1. Introduction

Alzheimer's disease (AD) accounts for 50–60% of all dementing illnesses (Blennow et al., 2006), with incidence rates doubling every 5 years after the age of 65. It is estimated that half of the population above 80 years old may have symptomatic AD, and that this number will grow rapidly as life expectancy increases. The psychological and financial cost of AD is tremendous and rapidly rising. There is currently no disease-modifying treatment, and many potential treatments being tested may have significant side effects. A recent upsurge of interest has been directed toward developing both diagnostic and prognostic biomarkers that can predict which individuals are relatively more likely to progress clinically.

AD is a neurodegenerative disorder characterized by significant impairments in multiple cognitive domains including memory, attention, reasoning, language and executive-functions. The pattern of brain pathology in AD evolves as the disease progresses — starting mainly in the hippocampus and entorhinal cortex, and subsequently spreading throughout most of the temporal lobe and the posterior cingulate, finally involving extensive brain regions (Braak and Braak, 1996; Jack et al., 2005; Thompson and Apostolova, 2007). Earlier neuroimaging studies investigating the neuromechanisms of AD usually have focused on focal activation abnormalities in individual brain regions, such as the medial temporal lobe (MTL) and posterior regions (Dickerson and Sperling, 2005). However, alterations in functional integrations of distributed brain systems in AD patients have recently attracted more investigative attention. Studies in neuropathological, electrophysiological, and neuroimaging domains indicate that cognitive dysfunctions in AD are not only associated with abnormalities in specific brain regions but also may reflect functional disconnections between widespread brain areas; these findings have led to the disconnection theory of AD (Delbeuck et al., 2003). It is particularly noteworthy that several studies using graph theoretical approaches consistently detect AD-related topological changes compared with normal controls in whole brain networks, especially losses of small-world attributes characterized by abnormal clustering coefficients and characteristic path lengths, providing additional evidence for the disconnection theory of AD (He et al., 2009). It has been shown

* Corresponding author at: Institute of Automation, Chinese Academy of Sciences P.O. Box 2728, Beijing, 100190, China. Tel.: +86 10 82618465; fax: +86 10 62527995.
E-mail address: tian@ieee.org (J. Tian).
[1] The authors contributed equally to this work.

0925-4927/$ – see front matter © 2012 Elsevier Ireland Ltd. All rights reserved.
doi:10.1016/j.pscychresns.2012.03.002

that declines in multiple cognitive domains in AD patients accompany weakened local or global information-transferring abilities in whole brain networks.

As the prodromal stage of AD, mild cognitive impairment (MCI) refers to the clinical condition that is intermediate between normal aging and AD. MCI patients usually experience memory loss to a greater extent than one would expect for individuals of their age, but they do not meet the full criteria for AD (Petersen et al., 1999). According to a previous study, nearly half of MCI patients will convert to AD in 5 years (Petersen et al., 2001). It is thus necessary to explore the neurological relations between AD and MCI, for such an exploration may result in opportunities for relatively early diagnosis of AD. A pathological study (Braak et al., 1999) has shown that neurodegeneration in AD begins in the MTL (including the hippocampus, amygdala, and parahippocampal gyrus), while a neurological study (Petersen et al., 2001) finds that the MTL exhibits abnormalities in MCI patients as well. Furthermore, Agosta et al. (2010), in a study investigating the brain motor network during a simple motor task, find that the functional connectivity is altered between primary sensorimotor cortices in MCI patients, suggesting the occurrence of a widespread brain rewiring rather than a specific response of a cognitive network. A recent study explores the brain networks in MCI patients using structural magnetic resonance imaging (MRI) by measuring the gray matter volume and finds altered interregional correlations mainly in the MTL as well as the abnormal hub regions in the frontal lobe and the temporal lobe (Yao et al., 2010). It is still unclear, however, whether the global functional integrations of the whole brain networks are altered in MCI patients. Even if the answer is positive, the manifestations of the relationship between MCI and AD in the topological organization of whole brain networks need to be addressed.

The "small world", characterized by large clustering coefficients and short characteristic path lengths, is an attractive model to describe both local and global information processing within complex brain networks (Bullmore and Sporns, 2009). Moreover, it provides quantitative parameters to measure the connectivity of brain networks (Bassett and Bullmore, 2006). Recent studies using the electroencephalogram (EEG) (Stam et al., 2007) and MRI (He et al., 2008; Yao et al., 2010) have found abnormal clustering coefficients and characteristic path lengths in the brain networks of AD patients, implicating a loss of small-world attributes and disrupted whole brain network architectures in those suffering from AD. Few studies, however, have examined the characteristics of whole brain networks in MCI patients.

In this study, we attempted to investigate the topological properties of whole brain networks in AD patients and MCI patients in comparison with age-matched normal controls using graph theoretical approaches. The main hypotheses were as follows:

(1) Several previous studies have indicated losses of small-world attributes in AD patients (e.g., He et al., 2009). It is possible that such topological changes also exist in the functional brain networks in MCI patients. In this study, we hypothesized that both AD and MCI would be characterized by altered small-world parameters in large-scale functional brain networks.
(2) As MCI is viewed as the intermediate stage between AD and normal aging, the disruptions in MCI are expected to be less severe than those in AD. We hypothesize that measures of brain networks in MCI patients will lie between those of AD patients and normal controls, and we also expect to demonstrate differences among AD patients, MCI patients and normal controls.
(3) Recent studies of AD and MCI have shown that brain regions in the MTL are where neurodegeneration begins (Braak et al., 1999; Petersen et al., 2001; Dickerson and Sperling, 2005). We hypothesized that nodal centrality changes in these regions will be detected in AD and MCI patients compared with normal controls, as well as between AD and MCI groups.

2. Methods

All research procedures were approved by the Tiantan Hospital Subcommittee on Human Studies and were conducted in accordance with the Declaration of Helsinki.

2.1. Subjects

From Beijing Tiantan Hospital, we recruited 16 right-handed subjects with MCI and 18 right-handed subjects with AD, according to the MCI criteria (Petersen et al., 1999, 2001) and the National Institute of Neurological and Communicative Disorders and Stroke-Alzheimer's Disease and Related Disorders Association (NINCDS-ADRA) criteria (McKhann et al., 1984). Eighteen healthy right-handed age-matched subjects served as controls. Before the experiment, the purpose of the study was briefly explained to the subjects. Each subject provided written informed consent approved by Institutional Review Board of the Tiantan Hospital Subcommittee on Human Studies. Control subjects were excluded if they had any neurological or psychiatric illness, or if they were taking medications or other substances that would influence the central nervous system (Table 1).

2.2. Data acquisition and preprocessing

All experiments were performed on a Siemens Trio 3-Tesla MRI system at Tiantan Hospital. A custom-built head holder was used to prevent head movements. The resting state scan lasted for 500 s. Functional MR images were obtained using a gradient echo T2*-weighted pulse sequence with repetition time (TR) = 2000 ms, echo time (TE) = 30 ms, matrix = 64 × 64, field of view (FOV) = 256 mm × 256 mm, and flip angle (FA) = 85°. Then, 20 slices (6-mm thickness, no gap) oriented parallel to the anterior commissure/posterior commissure (AC-PC) line were collected to cover the whole brain. After the functional run, a high-resolution T1-weighted 3D MRI sequence was used (voxel size = 1 × 1 × 1 mm^3, no gap, TR = 2100 ms, TE = 3.25 ms, matrix = 256 × 256, FOV = 230 mm × 230 mm, and FA = 10°).

All preprocessing steps were carried out using Matlab 7.6.0 (R2008a) with Statistical Parametric Mapping software (SPM5). The first five volumes of each session were discarded to allow for equilibrations of the magnetic field. All the remaining volumes were firstly realigned to correct for head motions using the least-squares minimization. None of the subjects had head movements exceeding 2 mm on any axis or head rotations greater than 1°. Then, the imaging data were further processed with spatial normalization based on the Montreal Neurological Institute (MNI) space (Ashburner and Friston, 1999), and re-sampled at 2 mm × 2 mm × 2 mm. Temporal band-pass filtering (0.01 < f < 0.08 Hz) was performed to reduce the effects of low-frequency drifts and high-frequency noise (Fox et al., 2005). Finally, the images were smoothed with a 6-mm full-width at half-maximum (FWHM) Gaussian kernel.

2.3. Anatomical parcellation

After preprocessing, the fMRI data were segmented into 90 regions (45 for each hemisphere), using an anatomically labeled template (Tzourio-Mazoyer et al., 2002) that has been widely used in previous neuroimaging studies via graph theoretical approaches (Salvador et al., 2005; Achard et al., 2006; Achard and Bullmore, 2007). For each subject, the representative time series of each region was estimated simply by averaging the fMRI time series over all voxels in the region.

2.4. Graph construction

We calculated partial correlations between each pair of brain regions to reduce the indirect dependencies by other brain regions and to obtain a partial correlation matrix R (Salvador et al., 2005). Then, we applied Fisher's transform to improve the normality of the partial correlation coefficients. Finally, a threshold (r) was related with the partial correlation coefficient (R_{ij}) to convert R to a binary graph. In this step, we set any R_{ij} whose absolute value was greater than r to 1 and others to 0. And a false discovery rate

Table 1
Subject characteristics.

	AD	MCI	Controls
N	18	16	18
Age range (year)	(43–76)	(54–81)	(49–78)
Age (mean ± S.D.)	63.7 ± 8.6	68.5 ± 9.4	64.9 ± 8.4
Sex(M/F)	9/9	9/7	10/8
MMSE score (mean ± S.D.)	17.1 ± 2.8	24.8 ± 1.3	29.5 ± 0.5
CDR	1	0.5	0

No significant between-group differences ($p < 0.05$) were observed in age, sex between groups. Significant differences were noted in MMSE scores between groups ($p < 0.0001$).
MMSE: Mini-Mental State Examination, CDR: Clinical Dementia Rating.

(FDR) procedure was performed at a q value of 0.05 to adjust for multiple comparisons (Genovese et al., 2002).

When the same threshold was applied to the matrices of the three groups, the resulting graphs would be composed of different numbers of edges. Thus, the between-group differences in network parameters would not reflect the alterations of topological organizations precisely. To control this effect, we converted the correlation matrix of each group to a binary graph with the same number of edges (Achard and Bullmore, 2007; Stam et al., 2007) or a fixed sparsity (S) defined as the number of edges in a graph divided by the maximum possible number of edges of the graph (He et al., 2008). Because there is no gold standard to select a single threshold, we thresholded each correlation matrix repeatedly over a wide range of sparsity ($8\% \leq S \leq 36\%$) and calculated the parameters of the resulting graphs with different thresholds.

2.5. Small-world analysis

Small-world measures of the functional connectivity of nervous systems involve clustering coefficients, C_p, and characteristic path length, L_p (Watts and Strogatz, 1998). C_p is the averaged clustering coefficient over all the nodes in the graph. The clustering coefficient of a node is the ratio of the number of existing connections among the neighbors of the node to the number of all possible connections. C_p measures the extent of local efficiency of information transfer of a network (Watts and Strogatz, 1998; Latora and Marchiori, 2001). L_p is the average of the shortest path lengths between any pair of nodes in the graph (Watts and Strogatz, 1998). However, when the networks consist of more than one component, this original definition is problematic for the existing nodal pairs with no connections. To avoid this problem, L_p was measured in this study by using a "harmonic mean" distance between nodal pairs (Newman, 2003). L_p measures the global efficiency of the brain network (Latora and Marchiori, 2001).

In order to determine whether the experimental networks have small-world attributes, a comparison must be made to random networks with the same number of nodes and average degree. Random networks with a Gaussian degree distribution will have clustering coefficients given by $C_p^{rand} = <k>/N$ ($<k>$ is the average degree of the network and N is the total number of nodes) (Albert and Barabási, 2002). The path lengths of a random network are given by $L_p^{rand} = \ln N / \ln(<k>)$ ($<k>$ is the average degree of the network and N is the total number of nodes) (Albert and Barabási, 2002). A real network is considered to have the small-world topology if it meets the criteria: $\gamma = C_p^{real}/C_p^{rand} > 1$ and $\lambda = L_p^{real}/L_p^{rand} \sim 1$ (Watts and Strogatz, 1998).

2.6. Nodal centrality

In this study, we considered the "betweenness centrality" of the nodes in the networks to investigate nodal characteristics. The betweenness B_i of a node i was defined

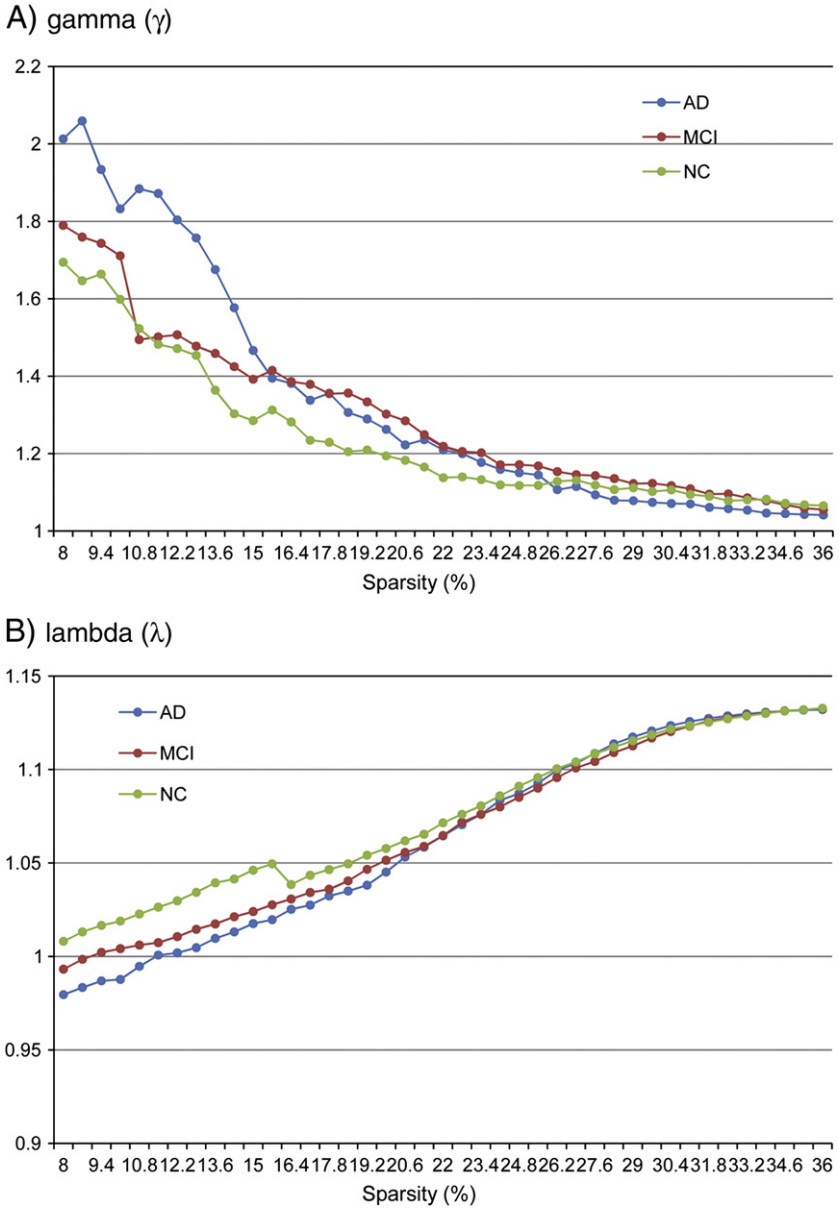

Fig. 1. Small-world properties for AD, MCI and normal control subjects.The graphs show the γ (C_p^{real}/C_p^{rand}, upper) and λ (L_p^{real}/L_p^{rand}, lower) in normal controls, AD patients and MCI patients as a function of sparsity thresholds. Among a wide range of degrees of sparsity, all networks have $\gamma > 1$ and $\lambda \approx 1$ demonstrating prominent small-world properties (see Section 2). As the sparsity increases, the γ decreases rapidly, whereas the λ increases slightly.

as the number of shortest paths between any pair of nodes that run through node i (Freeman, 1977). We considered the normalized betweenness $b_i = B_i/<B>$ ($<B>$ was the average betweenness of the network) as in He et al. (2008). The brain regions with high values of b_i were considered to be the hubs of the brain networks. The differences in b_i may reflect the changes of the brain network topology caused by the diseases.

2.7. Statistical analysis

We used a nonparametric permutation test to investigate the statistical significance of the between-group differences in the two characteristics of the whole brain networks, L_p and C_p. First, we calculated the C_ps and L_ps of the real networks at a given sparsity for each of the three groups, respectively. To test whether the observed group differences could occur by chance, we put the data of AD patients and normal controls together. Then, we randomly chose some subjects of the new group to be considered as AD patients and the rest as normal controls. The number of supposed AD patients was equal to the number of actual patients in the original group. We then calculated the differences between the new groups and repeated this process 1000 times. In each of the 1000 cases, we used the same sparsity threshold to generate corresponding binarized matrices and computed the L_p and C_p for each of the randomized groups, obtaining the between-group differences. We sorted the 1000 recorded differences and observed whether the between-group differences in the real networks were contained within 95% (two-tailed) of the supposed between-group differences. If they were, we accepted the null hypothesis that the two groups had identical probability distributions at the 0.05 significance level; otherwise we rejected the null hypothesis. This permutation test procedure was repeated at the sparsity of $8\% \leq S \leq 36\%$. This same procedure was repeated comparing MCI with AD groups and comparing normal controls with MCI groups.

3. Results

3.1. Small-world model and alterations related to AD and MCI

In this study, we examined the small-world attributes of the resting state networks in AD patients, MCI patients, and age-matched normal controls. The λ and γ of the networks illustrated the function of sparsity (Fig. 1). When the sparsity increased, the γ in all the three networks fell down, while the λ increased. Compared with matched random networks, all networks demonstrated small-world architectures as they all had almost identical characteristic path lengths ($\lambda \approx 1$) but were more locally clustered ($\gamma > 1$) over a wide range of sparsity ($8\% \leq S \leq 36\%$). These findings are consistent with those of previous studies that found the human

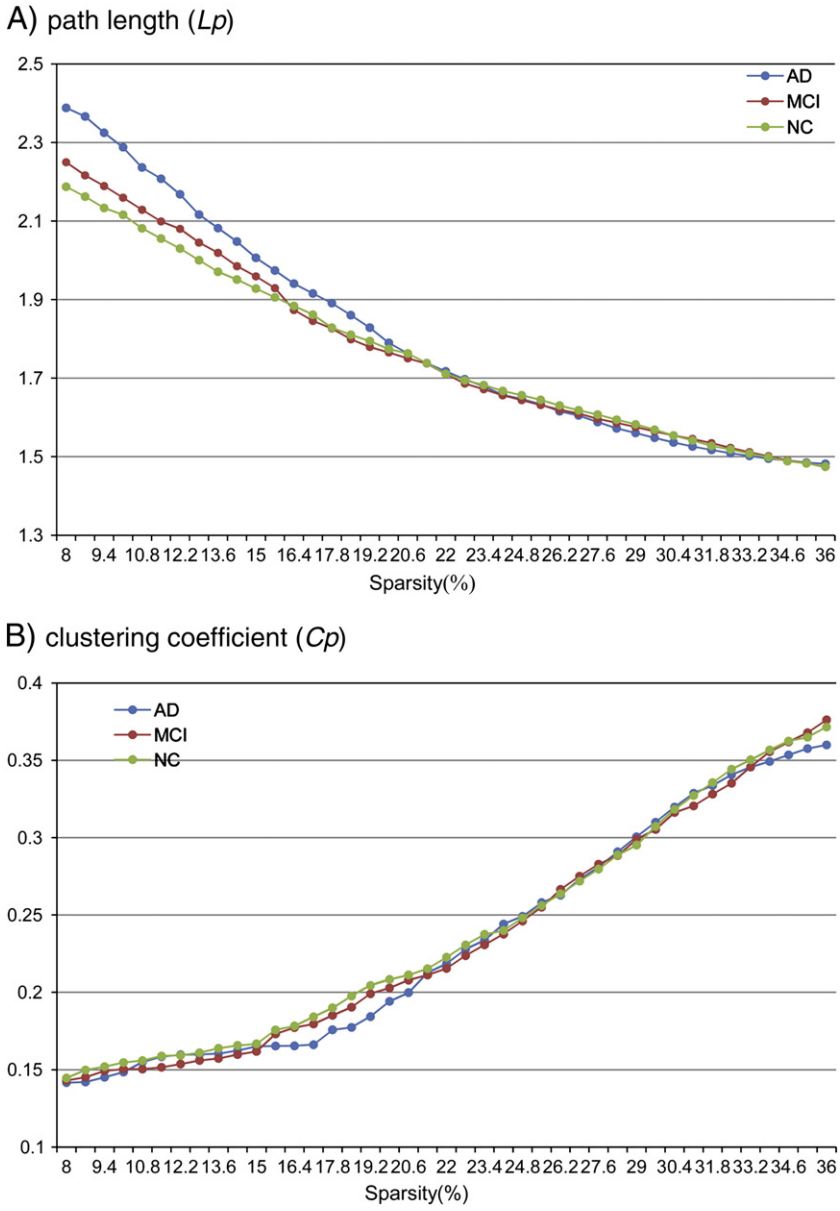

Fig. 2. Characteristic path lengths and clustering coefficients of the whole brain networks in AD, MCI and normal control subjects.The graphs show the characteristic path lengths (L_p, upper) and clustering coefficients (C_p, lower) in normal controls, AD patients and MCI patients as a function of sparsity thresholds. The C_p was the greatest for AD over the entire range of sparsity. The L_p was the greatest for AD over a wide range of sparsity. Both the two measures of MCI were intermediate between those of NC and AD.

brain to be an efficient neural architecture (Bullmore and Sporns, 2009). At low sparsity, the γ of AD networks was the largest in the three groups, while the λ of AD networks was the smallest. Both measures of MCI patients' networks were intermediate within the three groups.

To further study the alterations of small-world attributes in AD and MCI groups compared with normal controls, we examined clustering coefficients, C_p, and characteristic path lengths, L_p (Fig. 2). We found that the L_p decreased while the C_p increased as a function of sparsity in all three groups. Both L_p and C_p in the AD networks were the greatest in the three groups. Additionally, the two measures of MCI networks were intermediate in the three groups. A nonparametric permutation test was used to reveal significant statistical between-group differences of the L_p and C_p. In Fig. 3, significant differences ($p<0.05$) was detected in L_p at $8\% \leq S \leq 15\%$, and in Cp at $8\% \leq S \leq 26\%$ between AD and controls. While significant differences ($p<0.05$) between AD and MCI in L_p were detected at $8\% \leq S \leq 11\%$, we found no significant differences for L_p and C_p between MCI and controls. There was also no significant difference between AD and MCI for the C_p. Our findings that the L_p increased in AD compared with MCI suggested that AD patients had a further loss of small-world attributes as compared with MCI patients.

3.2. Nodal characteristics and alterations related to AD and MCI

The networks were constructed at the sparsity of 9%, which ensured all nodes included in the networks to present the nodal characteristics of the networks. The brain regions with $b_i > 1.7$ were identified as the hubs of the networks, symbolizing that the betweenness of the hubs was over 1.7 times larger than the average betweenness of the network. In this study, 14 brain regions were identified as hubs in the three groups, respectively (Table 2).

Finally, we examined the changes of the betweenness centrality in the AD and MCI patients. Compared with healthy controls, MCI patients showed centrality decreases in the brain areas of the angular gyrus, Heschl's gyrus, hippocampus and superior parietal gyrus, while the centrality increases were in the brain areas of the calcarine, inferior occipital gyrus and superior frontal gyrus (Table 3 and Fig. 4A). Compared with AD patients, MCI patients showed the centrality decreases mainly in the brain areas of the amygdala and rolandic operculum, and the centrality increases primarily in the brain areas of Heschl's gyrus, inferior parietal gyrus, middle frontal gyrus, parahippocampal gyrus, and precuneus (Table 3 and Fig. 4B).

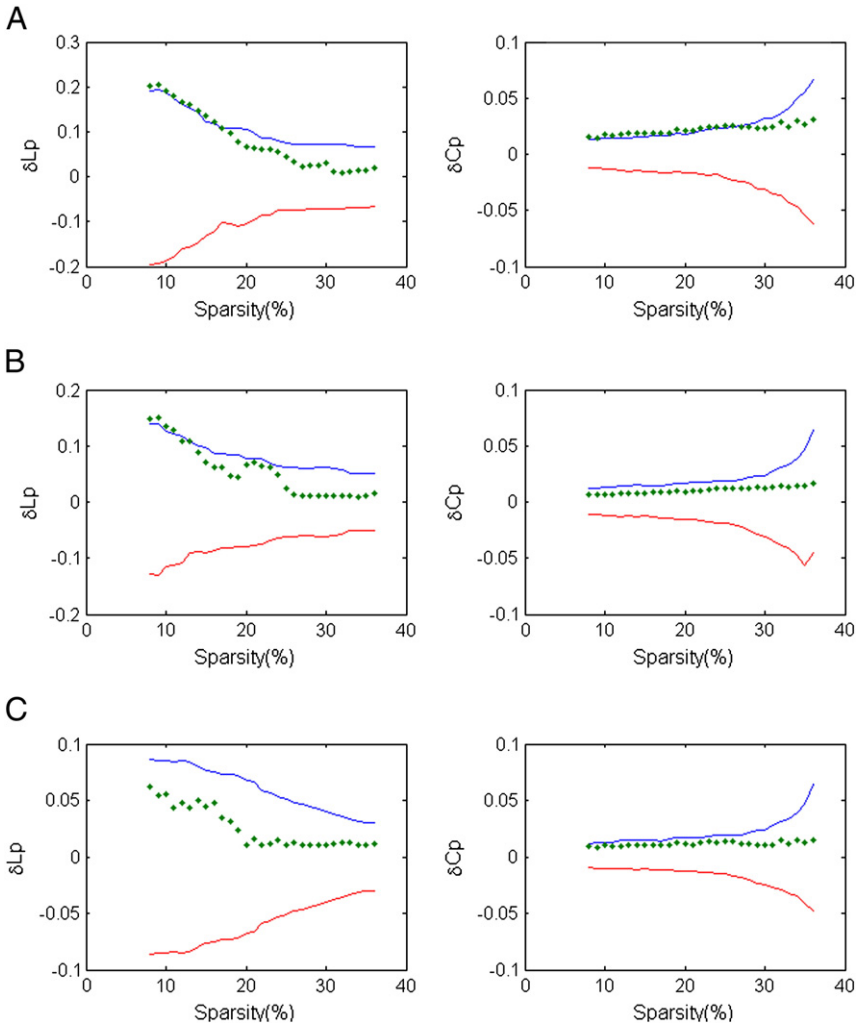

Fig. 3. Between-group differences in the characteristic path lengths and the clustering coefficients over a range of sparsity.The left panel shows the between-group differences in the characteristic path lengths (δL_p), and the right panel shows the between-group differences in the clustering coefficients (δC_p) over a wide range of sparsity ($8\% \leq S \leq 36\%$). The blue and red lines represent the 95% confidence intervals of the between-group differences obtained from 1000 permutation tests at each sparsity.A. Differences between the AD and NC groups ($\delta L_p = L_{pAD} - L_{pNC}$, $\delta C_p = C_{pAD} - C_{pNC}$).B. Differences between the AD and MCI groups ($\delta L_p = L_{pAD} - L_{pMCI}$, $\delta C_p = C_{pAD} - C_{pMCI}$).C. Differences between the MCI and NC groups ($\delta L_p = L_{pMCI} - L_{pNC}$, $\delta C_p = C_{pMCI} - C_{pNC}$).

Table 2
Regions showing high betweenness in brain networks.

Regions	Normalized betweenness, b_i	Degree, k_i
A. Normal subjects		
Left amygdala	1.7369	9
Right angular	2.9828	15
Left heschl	1.8631	11
Left hippocampus	1.9714	11
Right middle frontal orbital	2.4754	11
Left middle temporal	2.4244	9
Left posterior cingulate gyrus	1.8877	10
Right precuneus	1.8107	8
Right rectus	1.7119	10
Right rolandic operculum	3.3124	13
Right superior parietal	3.4151	12
Left superior temporal	1.9818	9
Right superior temporal	2.5251	9
Right supramarginal gyrus	3.9165	15
B. MCI patients		
Left amygdala	3.8647	15
Left calcarine	3.0409	10
Right inferior occipital	3.1764	13
Right Inferior frontal orbital	3.4106	12
Left insula	2.4055	8
Left lingual	1.7986	12
Right middle temporal pole	2.0316	8
Right middle temporal	1.8901	7
Right rolandic operculum	2.6390	9
Left superior frontal gyrus, dorsolateral	4.4012	16
Right superior frontal gyrus, dorsolateral	1.9184	9
Right superior frontal gyrus, medial orbital	1.7238	9
Left superior frontal orbital	2.5894	11
Right superior frontal orbital	1.9703	9
C. AD patients		
Right anterior cingulate gyrus	2.2498	8
Left cuneus	1.8391	9
Left heschl	1.7062	8
Right inferior occipital	2.6482	10
Left inferior frontal orbital	2.6140	9
Right inferior parietal	4.3833	12
Left middle frontal orbital	1.8949	9
Left middle frontal	4.5495	7
Right middle frontal	1.8472	12
Right parahippocampal	3.5775	11
Left postcentral	2.1778	8
Left precuneus	2.4543	10
Left superior occipital	2.0626	8
Right supramarginal gyrus	1.7587	9

Table 3
Regions showing significant difference.

A. Between MCI patients and normal controls in the nodal centrality

Regions	Normalized betweenness, b_i	
	MCI	NC
Decreased related to MCI		
Left heschl	0.1538	1.8631
Right angular	0.7229	2.9828
Left hippocampus	0.3206	1.9714
Right superior parietal gyrus	0.9737	3.4151
Increased related to MCI		
Left calcarine	3.0409	0.4858
Right inferior occipital gyrus	3.1764	0.2239
Left superior frontal gyrus, dorsolateral	4.4012	0.1000

B. Between MCI patients and AD patients in the nodal centrality

Regions	Normalized betweenness, b_i	
	MCI	AD
Decreased related to AD		
Left amygdale	3.8647	0.6699
Right rolandic operculum	2.6390	0.5415
Increased related to AD		
Right inferior parietal gyrus	0.7890	4.3833
Left middle frontal gyrus	0.8725	4.5495
Right parahippocampal	0.1876	3.5775
Left precuneus	0.3056	2.4543

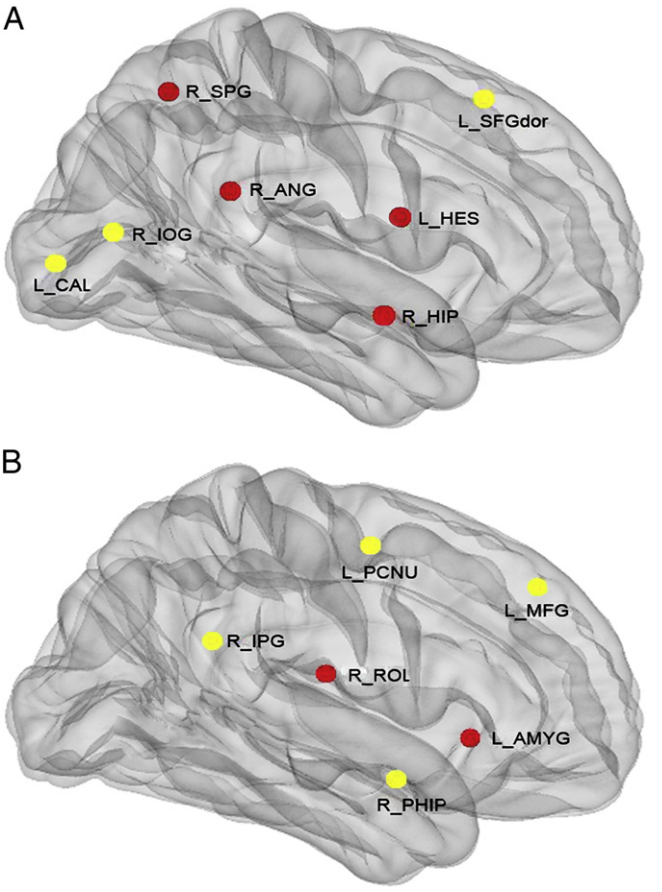

Fig. 4. Brain regions showing abnormal nodal centrality in whole brain networks.A. Regions showing decreased (red) and increased (yellow) nodal centrality in MCI patients compared with healthy control subjects.B. Regions showing decreased (red) and increased (yellow) nodal centrality in AD patients compared with MCI patients.(L_HES—left Heschl's gyrus, R_ANG—right angular, R_HIP-right hippocampus, R_SPG—right superior parietal gyrus, L_CAL—left calcarine, R_IOG—right inferior occipital gyrus, L_SFGdor—left superior frontal gyrus dorsolateral, L_AMYG—left amygdale, R_ROL—right rolandic operculum, R_IPG—right inferior parietal gyrus, L_MFG—left middle frontal gyrus, R_PHIP—right parahippocampal, L_PCNU—left precuneus).

4. Discussion

In this study, we investigated the topological properties of the whole brain networks in AD patients and MCI patients, compared with the age-matched healthy subjects. After searching in PubMed, we found that this was the first study to explore the topology of whole brain networks that comprised MCI patients, AD patients, and age-matched normal controls. The main findings of our study were as follows: (1) both MCI and AD patients exhibited losses of small-world attributes indicated by longer characteristic path lengths and larger clustering coefficients, (2) the properties of whole brain networks in the MCI patients ranged between those of normal subjects and AD patients, and (3) abnormal nodal centrality changes were detected in the brain networks in MCI patients compared with normal controls, and in AD patients compared with MCI patients.

The results demonstrated that the functional brain networks of AD patients, MCI patients and normal controls all showed small-world attributes. Previous studies have reported that the human brain has evolved into a complex but efficient neural architecture to maximize the power of information processing for the large clustering coefficients but short characteristic path lengths in whole brain networks

(Sporns and Zwi, 2004; Kaiser and Hilgetag, 2006). However, we detected that both AD and MCI patients showed longer characteristic path lengths and larger clustering coefficients over a wide range of sparsity. The L_p and C_p indicated global and local functional integration of whole brain networks that constitute basic cognitive processes (Sporns and Zwi, 2004). The increases of L_p and C_p in AD and MCI patients may represent disrupted information processing among distant brain regions across the whole brain, providing additional support to the disconnection theory of AD (Delbeuck et al., 2003). Using a non-parametric permutation test, we observed statistically significant differences in characteristic path lengths and clustering coefficients between AD patients and normal controls ($p<0.05$). The results that the L_p and C_p increased in AD patients compared with normal controls were consistent with those of previous studies that used structural MRI (He et al., 2008; Yao et al., 2010). We also detected significant differences in characteristic path lengths between MCI patients and AD patients ($ps<0.05$). But we found no significant differences in the two measures between normal controls and MCI patients, or in clustering coefficients between MCI and AD patients over the entire range of sparsity. These results indicated that the disruptions in the MCI networks were not so severe as that in the AD networks. And the findings may suggest that MCI patients form a boundary between normal aging and AD (Yao et al., 2010).

In addition, we noted that MCI patients showed decreased nodal centrality in several heteromodal association cortex regions (e.g., Heschl's gyrus and hippocampus) and increased nodal centrality mainly in frontal regions compared with the normal controls. The decreased nodal centrality in Heschl's gyrus could result from the development of MCI, because it has been demonstrated that Heschl's gyrus does not degenerate in normal aging (Chance et al., 2006). The hippocampus plays an important role in the development of AD and MCI. Previous studies have found that MCI patients had a significant reduction in the amount of gray matter in the hippocampus (Chetelat et al., 2002, 2005). Other studies observed reductions in the functional connectivity of the hippocampus to the regions of the default mode network in the very early stage of AD (Wang et al., 2006). Meanwhile, recent studies suggest that the hippocampus is likely to show abnormalities at the onset of AD before other brain regions are affected by the disease (Delbeuck et al., 2003). Therefore, we speculated that the abnormalities in these brain regions may cause cognitive declines greater than one could expect for age, and disrupt the topology of the whole brain network. In a previous study, the frontal areas were found to show increased functional connectivity to the regions of the default mode network in MCI (Bai et al., 2009), and this evidence is interpreted as the compensation for the loss of cognitive function in other brain regions (Grady et al., 2003). The results identified significantly increased functional connectivity at resting state in frontal regions, providing support to the previous studies.

Compared with AD patients, MCI patients showed decreased nodal centrality in the amygdala and rolandic operculum and increased nodal centrality in the frontal gyrus, parietal gyrus and MTL. Previous studies suggest that neuropathological changes in the amygdala may be linked to memory loss (Gallo et al., 2010); the reduction in the volume and thicknesses of the amygdala would predict conversions from the MCI to AD (Liu et al., 2010). A recent study found that the activities of the frontal and parietal gyrus were increased in MCI patients (Qi et al., 2010), indicating that these two regions may play more important roles in the brain networks of MCI patients. AD usually starts in the MTL (Dickerson and Sperling, 2005), and this region would degenerate as the disease progresses. Dickerson et al. (2005) pointed out that the MTL shows increased activity in MCI compared with AD. The brain regions showing decreased nodal centrality in AD compared with that in MCI might reflect the more serious functional degenerations in AD. We argue that these regional abnormalities may lead to rewiring in different brain systems and bring disruptions to the large-scale brain networks.

The recent literature examined in this review has strongly suggested that AD patients are characterized by disrupted functional and structural integrity in multiple distributed neuronal networks as well as in the whole brain system, which offers the promise of enhancing our understanding of the underlying disease mechanism in AD. However, we should acknowledge that the studies of complex brain networks in AD, as well as in normal subjects, are in very early stages. There are still a number of unanswered questions in this research field. Fourthly, the literature reviewed here strongly suggested that both AD and MCI (a higher risk for converting to AD) patients had abnormal neuronal integrity; however, it is unknown how the topological organization of brain networks alters at the conversion stage as disease progresses. Longitudinal studies will be helpful to clarify this issue. In addition, it would also be interesting to look at whether the carriers of the APOE-4 gene (a genetic risk factor for AD) show similar changes in their neuronal networks as previously demonstrated in AD.

In conclusion, the current investigation adopted graph-based analysis to study the whole brain network manifestation of neurological dysfunctions in MCI patients and AD patients compared with normal controls. Our results strongly suggested that both MCI patients and AD patients evidenced topological abnormalities in whole brain networks, particularly losses of small-world attributes and abnormal nodal centralities. However, this study is still at its initial stage. It is unknown how the topological organization of brain networks alters at the conversion stage as dementing disease progresses. Longitudinal studies will be helpful to clarify this issue. We could investigate the topological properties of the brain networks in MCI patients who converted to AD as compared with stable MCI patients in an attempt to identify those MCI patients with increased risk of progression to AD. In addition, we need to construct multi-resolution networks and integrate multi-level network features to fully understand the complex brain networks in MCI and AD, and attempt to find a new imaging-based biomarker of AD and MCI in the future.

Acknowledgments

This research is supported by the knowledge innovation program of the Chinese Academy of Sciences under grant no. KGCX2-YW-129, the Fundamental Research Funds for the Central University, the Beijing Nova program (Z111101054511116), the Project for the National Key Basic Research and Development Program (973) under grant nos. 2011CB707700, 2007CB512500, 2007CB512503, 2009CB521905, and the National Natural Science Foundation of China under grant nos. 81071137, 81071217.

References

Achard, S., Bullmore, E., 2007. Efficiency and cost of economical brain functional networks. PLoS Computational Biology 3, e17.
Achard, S., Salvador, R., Whitcher, B., Suckling, J., Bullmore, E., 2006. A resilient, low-frequency, small-world human brain functional network with highly connected association cortical hubs. Journal of Neuroscience 26, 63–72.
Agosta, F., Rocca, M.A., Pagani, E., Absinta, M., Magnani, G., Marcone, A., Falautano, M., Comi, G., Gorno-Tempini, M.L., Filippi, M., 2010. Sensorimotor network rewiring in mild cognitive impairment and Alzheimer's disease. Human Brain Mapping 31, 515–525.
Albert, R., Barabási, A.-L., 2002. Statistical mechanics of complex networks. Reviews of Modern Physics 74, 47–97.
Ashburner, J., Friston, K.J., 1999. Nonlinear spatial normalization using basis functions. Human Brain Mapping 7, 254–266.
Bai, F., Watson, D.R., Yu, H., Shi, Y., Yuan, Y., Zhang, Z., 2009. Abnormal resting-state functional connectivity of posterior cingulate cortex in amnestic type mild cognitive impairment. Brain Research 1302, 167–174.
Bassett, D.S., Bullmore, E., 2006. Small-world brain networks. The Neuroscientist 12, 512–523.
Blennow, K., de Leon, M.J., Zetterberg, H., 2006. Alzheimer's disease. Lancet 368, 387–403.
Braak, H., Braak, E., 1996. Evolution of the neuropathology of Alzheimer's disease. Acta Neurologica Scandinavica. Supplementum 165, 3–12.
Braak, E., Griffing, K., Arai, K., Bohl, J., Bratzke, H., Braak, H., 1999. Neuropathology of Alzheimer's disease: what is new since A. Alzheimer? European Archives of Psychiatry and Clinical Neuroscience 249 (Suppl. 3), 14–22.

Bullmore, E., Sporns, O., 2009. Complex brain networks: graph theoretical analysis of structural and functional systems. Nature Reviews Neuroscience 10, 186–198.
Chance, S.A., Casanova, M.F., Switala, A.E., Crow, T.J., Esiri, M.M., 2006. Minicolumn thinning in temporal lobe association cortex but not primary auditory cortex in normal human ageing. Acta Neuropathologica 111, 459–464.
Chetelat, G., Desgranges, B., De La Sayette, V., Viader, F., Eustache, F., Baron, J.C., 2002. Mapping gray matter loss with voxel-based morphometry in mild cognitive impairment. Neuroreport 13, 1939–1943.
Chetelat, G., Landeau, B., Eustache, F., Mezenge, F., Viader, F., de la Sayette, V., Desgranges, B., Baron, J.C., 2005. Using voxel-based morphometry to map the structural changes associated with rapid conversion in MCI: a longitudinal MRI study. NeuroImage 27, 934–946.
Delbeuck, X., Van der Linden, M., Collette, F., 2003. Alzheimer's disease as a disconnection syndrome? Neuropsychological Review 13, 79–92.
Dickerson, B.C., Sperling, R.A., 2005. Neuroimaging biomarkers for clinical trials of disease-modifying therapies in Alzheimer's disease. NeuroRx 2, 348–360.
Dickerson, B.C., Salat, D.H., Greve, D.N., Chua, E.F., Rand-Giovannetti, E., Rentz, D.M., Bertram, L., Mullin, K., Tanzi, R.E., Blacker, D., Albert, M.S., Sperling, R.A., 2005. Increased hippocampal activation in mild cognitive impairment compared to normal aging and AD. Neurology 65, 404–411.
Fox, M.D., Snyder, A.Z., Vincent, J.L., Corbetta, M., Van Essen, D.C., Raichle, M.E., 2005. The human brain is intrinsically organized into dynamic, anticorrelated functional networks. Proceedings of the National Academy of Sciences of the United States of America 102, 9673–9678.
Freeman, L.C., 1977. A set of measures of centrality based on betweenness. Sociometry 40, 35–41.
Gallo, D.A., Foster, K.T., Wong, J.T., Bennett, D.A., 2010. False recollection of emotional pictures in Alzheimer's disease. Neuropsychologia 48, 3614–3618.
Genovese, C.R., Lazar, N.A., Nichols, T., 2002. Thresholding of statistical maps in functional neuroimaging using the false discovery rate. NeuroImage 15, 870–878.
Grady, C.L., McIntosh, A.R., Beig, S., Keightley, M.L., Burian, H., Black, S.E., 2003. Evidence from functional neuroimaging of a compensatory prefrontal network in Alzheimer's disease. Journal of Neuroscience 23, 986–993.
He, Y., Chen, Z., Evans, A., 2008. Structural insights into aberrant topological patterns of large-scale cortical networks in Alzheimer's disease. Journal of Neuroscience 28, 4756–4766.
He, Y., Chen, Z., Gong, G., Evans, A., 2009. Neuronal networks in Alzheimer's disease. The Neuroscientist 15, 333–350.
Jack Jr., C.R., Shiung, M.M., Weigand, S.D., O'Brien, P.C., Gunter, J.L., Boeve, B.F., Knopman, D.S., Smith, G.E., Ivnik, R.J., Tangalos, E.G., Petersen, R.C., 2005. Brain atrophy rates predict subsequent clinical conversion in normal elderly and amnestic MCI. Neurology 65, 1227–1231.
Kaiser, M., Hilgetag, C.C., 2006. Nonoptimal component placement, but short processing paths, due to long-distance projections in neural systems. PLoS Computational Biology 2, e95.
Latora, V., Marchiori, M., 2001. Efficient behavior of small-world networks. Physiological Review Letters 87, 198701.
Liu, Y., Paajanen, T., Zhang, Y., Westman, E., Wahlund, L.O., Simmons, A., Tunnard, C., Sobow, T., Mecocci, P., Tsolaki, M., Vellas, B., Muehlboeck, S., Evans, A., Spenger, C., Lovestone, S., Soininen, H., 2010. Analysis of regional MRI volumes and thicknesses as predictors of conversion from mild cognitive impairment to Alzheimer's disease. Neurobiology of Aging 31, 1375–1385.
McKhann, G., Drachman, D., Folstein, M., Katzman, R., Price, D., Stadlan, E.M., 1984. Clinical diagnosis of Alzheimer's disease: report of the NINCDS-ADRDA work group under the auspices of Department of Health and Human Services Task Force on Alzheimer's Disease. Neurology 34, 939–944.
Newman, M.E.J., 2003. The structure and function of complex networks. SIAM Review 45, 167–256.
Petersen, R.C., Smith, G.E., Waring, S.C., Ivnik, R.J., Tangalos, E.G., Kokmen, E., 1999. Mild cognitive impairment: clinical characterization and outcome. Archives of Neurology 56, 303–308.
Petersen, R.C., Doody, R., Kurz, A., Mohs, R.C., Morris, J.C., Rabins, P.V., Ritchie, K., Rossor, M., Thal, L., Winblad, B., 2001. Current concepts in mild cognitive impairment. Archives of Neurology 58, 1985–1992.
Qi, Z., Wu, X., Wang, Z., Zhang, N., Dong, H., Yao, L., Li, K., 2010. Impairment and compensation coexist in amnestic MCI default mode network. NeuroImage 50, 48–55.
Salvador, R., Suckling, J., Coleman, M.R., Pickard, J.D., Menon, D., Bullmore, E., 2005. Neurophysiological architecture of functional magnetic resonance images of human brain. Cerebral Cortex 15, 1332–1342.
Sporns, O., Zwi, J.D., 2004. The small world of the cerebral cortex. Neuroinformatics 2, 145–162.
Stam, C.J., Jones, B.F., Nolte, G., Breakspear, M., Scheltens, P., 2007. Small-world networks and functional connectivity in Alzheimer's disease. Cerebral Cortex 17, 92–99.
Thompson, P.M., Apostolova, L.G., 2007. Computational anatomical methods as applied to ageing and dementia. British Journal of Radiology 80 (Spec No 2), S78–S91.
Tzourio-Mazoyer, N., Landeau, B., Papathanassiou, D., Crivello, F., Etard, O., Delcroix, N., Mazoyer, B., Joliot, M., 2002. Automated anatomical labeling of activations in SPM using a macroscopic anatomical parcellation of the MNI MRI single-subject brain. NeuroImage 15, 273–289.
Wang, L., Zang, Y., He, Y., Liang, M., Zhang, X., Tian, L., Wu, T., Jiang, T., Li, K., 2006. Changes in hippocampal connectivity in the early stages of Alzheimer's disease: evidence from resting state fMRI. NeuroImage 31, 496–504.
Watts, D.J., Strogatz, S.H., 1998. Collective dynamics of 'small-world' networks. Nature 393, 440–442.
Yao, Z., Zhang, Y., Lin, L., Zhou, Y., Xu, C., Jiang, T., 2010. Abnormal cortical networks in mild cognitive impairment and Alzheimer's disease. PLoS Computational Biology 6, e1001006.